Paper No. 1692. (quote when citing this article)
Eleventh World Conference on Earthquake Engineering
ISBN: 0 08 042822 3

THE SEISMIC BEHAVIOUR OF ELASTOMERIC AND LEAD-RUBBER BEARINGS

A. MORI
Earthquake Disaster Mitigation Department, Japan Engineering Consultants Ltd, Tokyo, Japan

P.J. MOSS, A.J. CARR and N. COOKE
Department of Civil Engineering, University of Canterbury, Christchurch, New Zealand

ABSTRACT

The experimental work covering a range of different sizes and hardnesses of seismic isolation bearings, considering both laminated elastomeric and lead-rubber bearings, was undertaken to investigate the stress distributions normal to the bearing faces as the shearing deformation was increased. The normal stress distributions show the degree of the bearing stability and, in the case of the Lead-Rubber bearing, illustrate a distinct difference between a well confined and a poorly confined lead plug in the bearings. Analytical investigations using the finite element method were carried out to verify the experimental bearing behaviour and to investigate the interaction between the rubber and steel shim layers in the bearings.

KEYWORDS

Shear, bearings, elastomeric bearings, lead-rubber bearings, seismic isolation, testing

INTRODUCTION

A large number of seismic isolation systems have been developed since the early 1970's. They are basically a combination of elastomeric bearings and energy dissipators such as lead-plugs, steel bars, steel springs, steel plate, and a combination of sliding bearings and re-centring devices. However, most of the studies on seismic-isolation systems have been related to energy dissipators, sliding bearings or the seismic-isolation itself. Elastomeric bearings play an important part in seismic isolation systems since they can lengthen the period of free vibration of a structure. The properties of elastomeric bearings have been investigated since 1940 in applications as bridge bearings and the existing design codes for elastomeric bearings are based on that research. This previous research work concerned the support of the dead and live loads by the compressive behaviour of the bearings, the understanding of the expansion and contraction of bridge decks due to temperature variations, and how these affect the lateral behaviour of bearings. The results of this research have been used also for the design of elastomeric bearings that form part of a seismic-isolation system. It seemed desirable therefore to investigate the current code requirements [AASHTO (1989); Standards Australia (AS1523, 1981); British Standards Inst. (BS5400, 1983); Highways Dir., Dept of Envir., Gt Br. (BE1/76, 1976); Ministry of Constr., Japan (1991); Ministry of Works & Devel. (MWD), NZ (1981a,b)] when the performance of the elastomeric bearings is examined as part of a seismic resistance system.

The experimental work described here and in the references by Mori [1993] and Mori *et al* [1995a,b] was

undertaken for both laminated elastomeric bearings (EB) and lead-rubber bearings (LRB) to obtain a better understanding of the real bearing behaviour under different types of deformation such as compression, shear and rotation. In particular, the investigation focused on the distributions of vertical pressure (normal stress) on the bearing faces and the degree of lift-off of the edges of the bearings as the shearing displacement and the angle of rotation increased.

The force-displacement response and normal stress distribution of the bearings in shear and rotation were determined by testing pairs of bearings in a specially developed self-equilibrating test frame using an Avery 1000 kN testing machine to apply an axial load and a double acting hydraulic jack to apply the shearing forces.

TEST PROGRAM

Five elastomeric bearing pairs and two lead-rubber bearing pairs were tested in the experimental program. Each pair was produced from the same batch of natural rubber and it was assumed that they would have identical properties. The principal plan dimensions of the selected bearings were 380 mm x 300 mm, with heights of 130 mm to 148 mm (see Table 1). The dimensions were similar to those normally used for bridge bearings in New Zealand and were the maximum dimensions that could be accommodated by the axial loading machine.

Table 1 Properties and Construction of the Bearings Tested

Bearing No.		1	2	3	5	6	7	8
Hardness degree for rubber		53	48	57	53	53	48	48
Construction								
no. of rubber inner layers		9	10	9	9	9	9	9
no. of steel shims (3 mm)[1]		10	10	8	8	8	8	8
no. of 10 mm outer steel plates[1]		-	1	2	2	2	2	2
size of lead plug (mm)		-	-	-	-	75	-	75
outer rubber thickness (mm)		5	4	5	5	5	5	5
side rubber cover thickness (mm)		7	10	10	10	10	10	10
total rubber thickness (mm)		100	108	100	100	100	100	100
total height of bearing (mm)		130	148	144	144	144	144	144
Shape factor	inner layer	6.6	7.9	7.9	7.9		7.9	
	outer layer	9.4	14.1	11.3	11.3		11.3	
Calculated stiffness[2]								
compression	(kN/mm)	125	170	258	222	-	182	-
shear	(kN/mm)	0.72	0.68	1.14	0.93	8.58[3] 1.32[4]	0.76	7.05[3] 1.08[4]
Applied maximum axial load (kN)		450	650	800	800	800	650	650

Note: 1) mild steel (Grade 250)
2) determined from BE1/76 for EB and CDP818/A for LRB
3) initial stiffness of the lead rubber bearing
4) post-elastic stiffness of the lead rubber bearing

The EB consisted of alternating 10 mm thick rubber inner layers and 3 mm thick steel shims with 10 mm thick steel outer plates and 5 mm thick rubber top and bottom cover layers. The LRB were of similar construction but with lead plugs of 75 mm diameter set into the centre of the bearing. The construction and properties of the bearings tested is summarised in Table 1. The bearing number 1, B1, was used for pretesting and to investigate the effect of plan dimension variation, these being 432 mm x 205 mm.

The design of EB was based on the British Department of the Environment Memorandum BE1/76 [High. Dir. (1976)] and the design of the LRB on the New Zealand Ministry of Works and Development (MWD) CDP 818/A [Min. Works & Dev. (1981a)]. The shape factors in Table 1 were calculated for the inner layers using the formula

$$\text{Shape factor, } S = \frac{L_e W_e}{2t_e\left(L_e + W_e\right)} \tag{1}$$

where L_e and W_e are the length and width respectively of the inner steel shims and t_e is the thickness of a rubber layer. For the outer layers, the equation in BE1/76 was used (i.e. the effective rubber thickness is estimated as 1.4 times the actual rubber thickness).

Test Rig and Instrumentation.

As shown in Fig. 1, a self-equilibrating frame was used to test a "back-to-back" double-bearing system in shear.

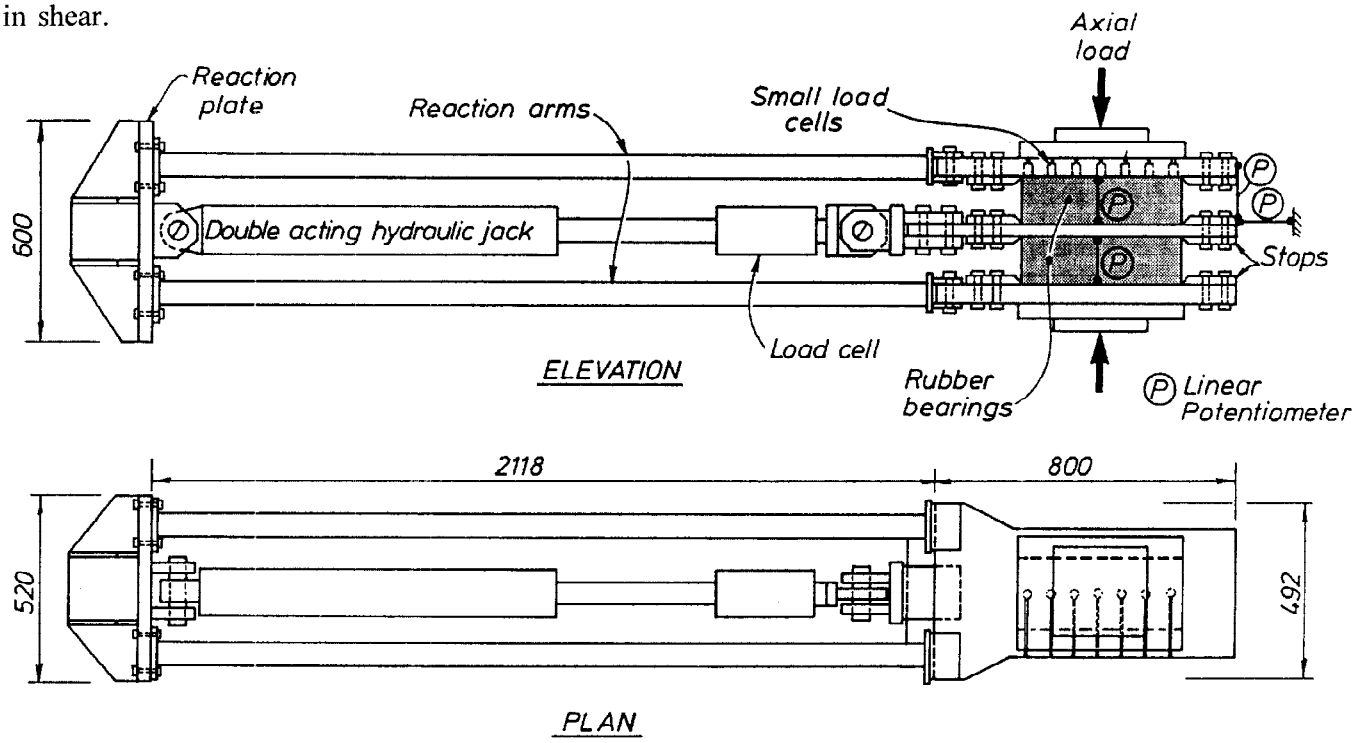

Fig. 1 Test rig used for the shear tests

An Avery 1000 kN capacity test machine was used to apply the axial loads and a double acting hydraulic jack applied the static cycling shearing forces via a load cell. The top and bottom platens of the axial loading machine were very rigid and the vertical movement of the system could be neglected. The hydraulic jack was connected to the centre plate and the reaction plate by pins at each end.

The pin connections at the ends of the hydraulic jack were set to follow the natural deformation of the bearings during the shear tests. The reaction arms were designed to be sufficiently flexible that bending moments were minimised when the bearings were compressed and the shearing deformation increased.

Two linear potentiometers for each bearing were centrally placed on both sides of the bearings to measure vertical deformations. One linear potentiometer was located at the back of the top bearing to measure vertical displacement of bearings so that the angle of rotation of the bearings due to the shearing force might be calculated. Two large linear potentiometers were fixed to the centre plate and were used to measure the relative shearing displacement of the bearings.

Stops constructed from pieces of steel plates with one chamfered edge at the face next to the bearings were bolted onto the loading plates in order to avoid slippage of the bearings on the loading plates. The outer rubber layers and outer steel plates of the bearings were constrained by these stops. Some codes recommend the use of dowels to retain bearings in position or to transmit shear forces. However, in situations where bearings need replacement, the use of dowels has made removal of the bearings difficult. Moreover, if dowels had been used in this test programme, their presence in the face of the bearing would have made it difficult to measure the vertical pressure distribution using the small load cells used for this purpose.

Small Load Cells (SLC).

A small load cell (SLC) was developed specially to measure the normal stress distribution on the top and bottom faces of the bearings. Each SLC consisted of a hollow cylinder 30 mm high and 20 mm diameter having a minimum wall thickness of 0.6 mm made from a high strength (800 MPa) steel.

The performance of the SLC was verified by examining the test results in terms of the vertical stress across Bearing 2 under an axial load of 650 kN [Mori (1993); Mori *et al* (1995a)]. It was found that the performance of the SLCs was reasonably reliable in terms of both the calculated reaction force and the shape of the measured normal stress distribution and the axial compression load.

EXPERIMENTAL INVESTIGATION

General trend of the stress distribution for EBs

Figure 2 shows the stress distributions that occur across the top face of Bearing 7 as the bearing shear strain increases from 0% to 150% for a compressive load of 440 kN (0.68W or 4.37 MPa where W = design axial load) and from 0% to 200% for compressive loads of 650 kN (1.0W or 6.45 MPa) and 800 kN (1.25W or 7.94 MPa). It can be seen from 0% bearing shear strain in the figure that the contact condition between the SLCs and the face of the bearing does not seem good for the low compressive load probably due to an inadequate amount of compressive load on the bearings. When the bearing shear strain reached about 125%, the normal stress at the bearing centre (SLC No. 4) started decreasing. Beyond this bearing shear strain, the change of the normal stress distribution rapidly progressed and lift-off of the bearing at 200% bearing shear strain occurred for nearly 50% (half of the bearing width) of the contact area between the bearing faces and the loading plates.

Normal stress distributions of well confined and poorly confined LRBs

The normal stress distribution across the top face of the LRB at 150% bearing shear strain under the design compressive load of 800 kN is shown in Fig. 3 together with the normal stress distribution of the EB having the same rubber hardness. As can be seen in the figure, the No. 3 SLC was in contact with both the lead plug and the rubber face. Therefore, the normal stress of the LRB at the SLC No. 3 was higher than that of the EB due to the boundary discontinuity between the lead plug and the rubber at the surface of the LRB. The effect of this discontinuity becomes more marked as the bearing shear strain increases and the deformation of the lead plug progresses. However, the normal stress distribution of the LRB at 0% bearing shear strain was similar to that of the EB [Mori (1993); Mori *et al* (1995a)]. After taking into account the discontinuity mentioned above, it was concluded that if the LRB was well confined by the appropriate compressive load, the normal stress distribution on the faces of the LRB could be generally regarded as being the same as those of the EB.

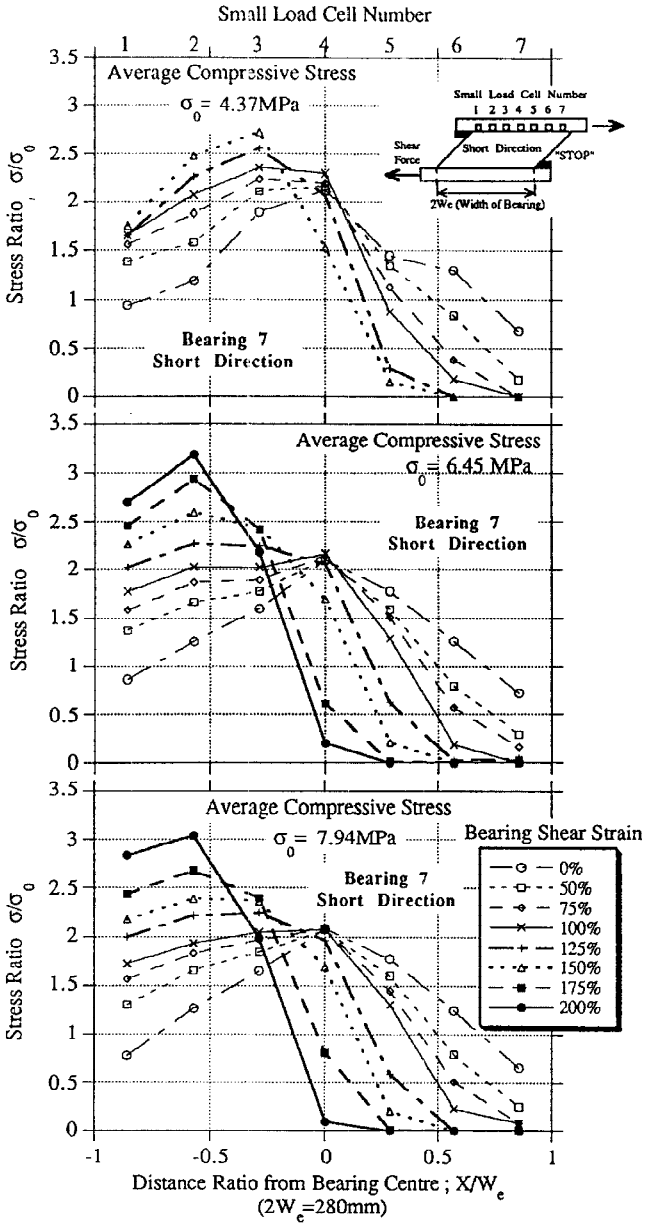

Fig. 2 Normal stress distribution across an EB as the bearing shear strain increases.

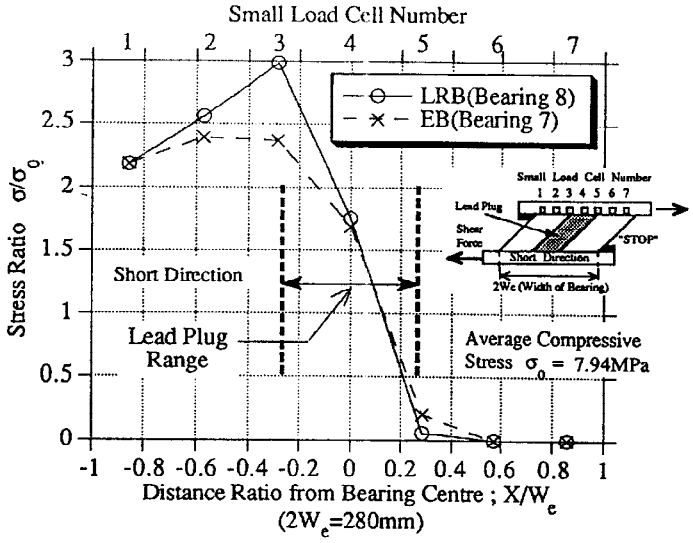

Fig. 3 Normal stress distributions of an EB and a well confined LRB under the design compressive load.

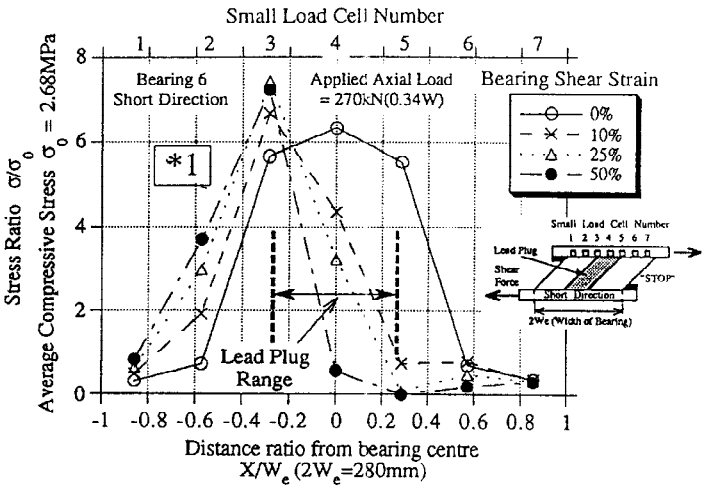

Fig. 4 Normal stress distributions of a poorly confined LRB under a compressive load of 270 kN.

Figure 4 shows the normal stress distributions of the LRB at the various bearing shear strains under a low compressive load of 270 kN. Because the LRB was confined by an inappropriate compressive load, the lead plug carried very high normal stress, about 6 to 7 times the average compressive stress at 0% to 50% bearing shear strain and this was very different from that shown under the high compressive load. These normal stress distributions were also different from those of the EB and showed that the effect of the boundary discontinuity between the lead plug and the rubber on the normal stress distributions of the LRB was even more significant for the case of low axial compression.

Figures 5 and 6 show the hysteresis loops corresponding to the well confined LRB of Fig. 3 and the poorly confined LRB of Fig. 4 respectively. It can be seen that the hysteretic action under the low compressive load is nonlinear during unloading whereas under the high compressive load the initial unloading behaviour is linear reflecting the behaviour of the lead plug. It seems that LRB need adequate compressive load to minimise the boundary discontinuity between the lead and rubber thus providing better confinement of the lead plug.

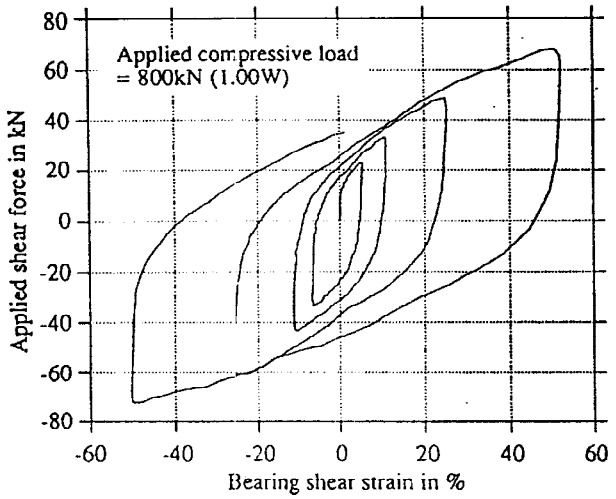

Fig. 5 Hysteresis loop of a well confined LRB.

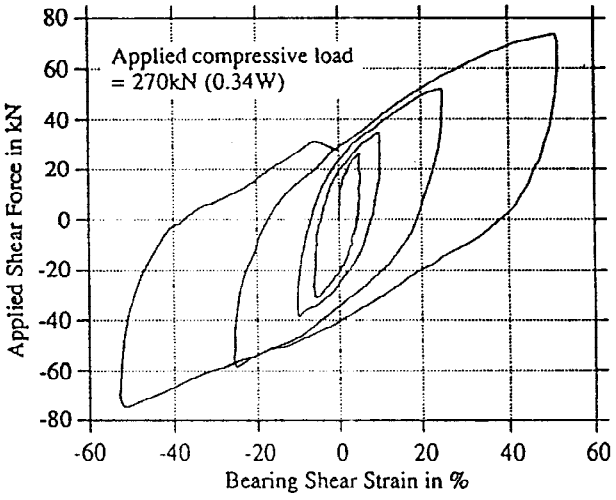

Fig. 6 Hysteresis loop of a poorly confined LRB.

ANALYTICAL INVESTIGATION

Modelling

The finite element method was used to analytically investigate the behaviour of the seismic isolation bearings. Bearing 7 (EB) was dealt with in this study. In the finite element analysis, the bearing was modelled by three dimensional solid elements. A rubber layer was modelled as two sub-layers using quadratic elements to efficiently model the bulging deformation at the edges and a steel shim plate was modelled by quadratic elements in one layer. The boundary between rubber layers and the steel shim plates was fixed as no bond failure was expected during the analysis from the observation of the experimental work. The top and bottom faces of the bearing were treated as frictional contact surfaces to model the real situation in the tests.

The rubber was assumed to be an incompressible non-linear elastic material and this was modelled mathematically using a strain energy functional that had a second order polynomial form fitted to data from a rubber sample tested in tension. The steel was treated as a rate independent elasto-plastic material and its elastic modulus and Poisson's ratio were assumed to be 200 GPa and 0.27 respectively. For the LRB, the lead in the plug was taken to be a perfectly plastic material with an elastic modulus of 17 GPa, Poisson's ratio of 0.44, and a yield stress of 3.0 MPa.

Analytical results

The above model was verified by comparing with the experimental results. Figure 7 shows the comparison of the shear force-deflection responses between the analysis and experiment under the design compressive load. Figure 8 shows the comparison of the normal stresses between the analysis and experiment at the bearing shear strains of 22% and 63% under the design compressive load. Both figures show that the analytical results are in reasonable agreement with the experimental values when the experimental error due to the imperfection of the test rig is considered. From those results, it was concluded that the model used in this study showed a satisfactory degree of accuracy. It was also found that stress in the steel shim plates near the bearing edges at the top and bottom faces of the bearing had almost reached the yield stress. The bearing deformation in shear was obtained from the analysis (Mori *et al*, 1993). The deformation of the elements near the bearing edges was very complicated so that numerical solutions could not be obtained beyond a bearing shear strain of 106% because of the difficulty of forming the stiffness matrix in the finite element analysis.

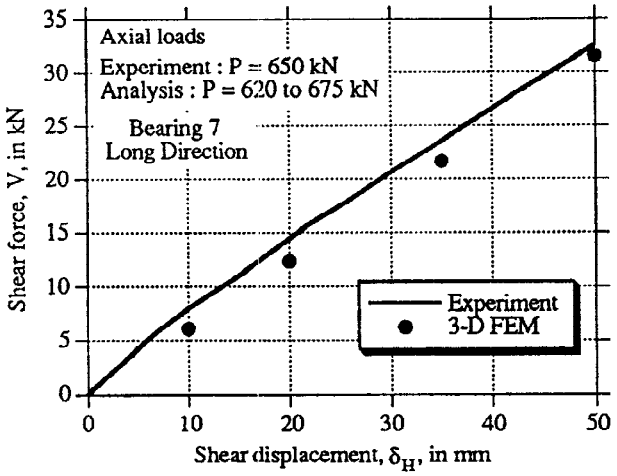

Fig. 7 Comparison of the shear force-deflection response of an EB between the analysis and experiment.

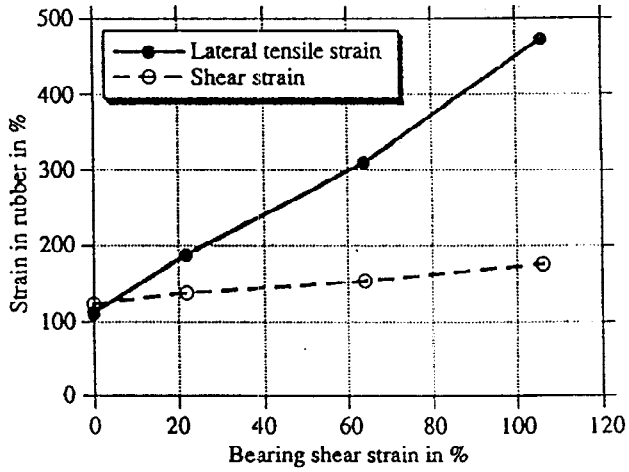

Fig. 9 Maximum lateral tensile and shear strains obtained between the first inner rubber layer and the outer steel plate versus bearing shear strains.

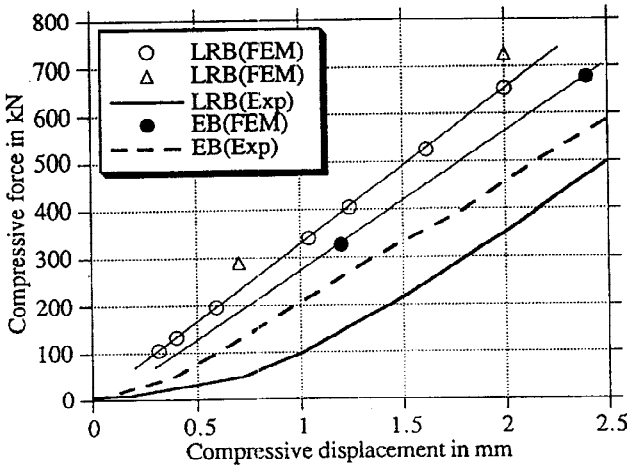

Fig. 10 Comparison of the compressive force-displacement responses from the analysis and experiment for the EB and LRB.

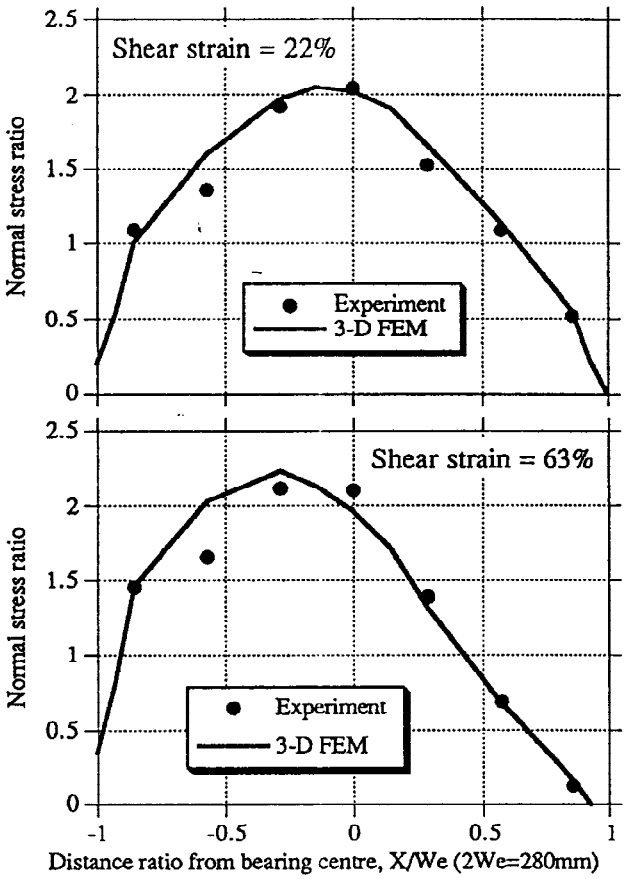

Fig. 8 Comparison of the normal stresses of an EB between the analysis and experiment at the bearing shear strains of 22% and 63% under the design compressive load.

Figure 9 shows the maximum lateral tensile strains and maximum shear strains at the interface between a rubber layer and a steel shim plate under shear loading. Both the lateral tensile and shear strains are increasing as the bearing shear strain increases. These maximum strains in at the interface were obtained near the bearing edges. The lateral tensile strain grows more rapidly than the shear strain. This is because the bulging deformation (outward projection) of rubber layers in the bearing becomes marked as the bearing shear strain increases.

The analytical model for the LRB was not completely satisfactory when compared with the experimental results on account of the excessive computational effort required. However, Fig. 10 shows a comparison of the compressive behaviour where it can be seen that the analytical and experimental slopes are similar.

CONCLUSIONS

The following conclusions can be drawn from the above investigations.

1. The normal stress across the bearing top face measured by the small load cell clearly showed the change of the bearing stability state.

2. The normal stress also showed the distinct difference between the well and poorly confined loading states of LRB.

3. The FEM model helps to explain the behaviour of the bearing in terms of the force-deflection response and the normal stress distributions on the bearing face observed in the tests.

4. The bulging deformation at the edges of the bearing introduced high tensile strains in the steel shims and high shear strains at the interface between an inner rubber layer and a steel shim.

5. The tensile strain grew more rapidly than the shear strain as the loading magnitude increased and the edge bulging effect became extremely marked as the loading level increased.

ACKNOWLEDGMENT

The authors would like to thank Skellerup Industrial Ltd. in Christchurch, New Zealand for their cooperation in testing the rubber samples. The computer program used for the finite element analysis was "ABAQUS" (1991) used under license from Hibbit, Karlsson and Sorensen Inc., USA. The financial support provided by Japan Engineering Consultants Co., Ltd. in Tokyo, Japan was much appreciated and is gratefully acknowledged.

REFERENCES

AASHTO (1989). *Standard Specifications for Highway Bridges*, 14th Edition, Washington DC, USA.

British Standards Institution (1983). BS5400: *Steel, Concrete and Composite Bridges, Parts 9A and 9B.*

Gent, A.N. (1963). Elastic Stability of Rubber Compression Springs, *Journal of Mechanical Engineering Science*, **6**,317-325.

Hibbit, Karlsson and Sorensen Inc. (1991). *ABAQUS* ver. 4.9, USA.

Highways Directorate, Dept of Environment, Great Britain (1976) *Design Recommendations for Elastomeric Bridge Bearings*, Technical Memorandum BE1/76.

Ministry of Construction, Japan (1991). *Guidelines for Design of Base-Isolated Highway Bridges*, Tokyo (in Japanese).

Ministry of Works and Development (MWD), New Zealand (1981a). *Design of Lead-Rubber Bridge Bearings*, Civil Engineering Division, CDP 818/A., Wellington, New Zealand.

Ministry of Works and Development (MWD), New Zealand (1981b). *Elastomeric Bearing Specification 81/12/22/2*, Wellington, New Zealand.

Mori, A. (1993). *Investigation of the Behaviour of Seismic Isolation Systems for Bridges*, PhD Thesis, University of Canterbury, Christchurch, New Zealand.

Mori, A., Moss, P.J. and Carr, A.J. (1993). *The Behaviour of Seismic Isolation Bearings*, Proc. Asia-Pacific Vibration Conference '93, Kitakyushu, Japan, **3**,1389-94.

Mori, A., Carr, A.J., Cooke, N. and Moss, P.J. (1995a). *The Compression Behaviour of Bearings Used for Seismic Isolation*, to be published in Engineering Structures.

Mori, A., Carr, A.J., Cooke, N. and Moss, P.J. (1995b). *The Behaviour of Bearings Used for Seismic Isolation Under Shear and Axial Load,* submitted to Earthquake Spectra.

Mori, A., Carr, A.J., Cooke, N. and Moss, P.J. (1995c). *The Behaviour of Bearings Used for Seismic Isolation Under Rotation and Axial Load,* submitted to Earthquake Spectra.

Standards Australia, AS1523-1981 (1981). *Elastomeric Bearings for Use in Structures.*